Leak Growth Mechanism in Composite Pd Membranes Prepared by the Electroless Deposition Method

Federico Guazzone and Yi Hua Ma
Center for Inorganic Membrane Studies, Chemical Engineering Dept., Worcester Polytechnic Institute, Worcester, MA 01609

DOI 10.1002/aic.11397
Published online December 28, 2007 in Wiley InterScience (www.interscience.wiley.com).

The leak (of He gas) in composite Pd membranes prepared by the electroless deposition method was studied. The leak was distributed over the entire surface of membranes, and was due to the formation of pinholes, 0.1–2 μm in dia., located at the boundaries of Pd clusters and Pd crystallites. The rate at which the leak developed in H_2 atmosphere was determined at 450, 500 and 550°C, and an apparent activation energy for the leak growth was calculated to be equal to 238 kJ/mol, which was close to the activation energy of Pd self-diffusion coefficient of 266 kJ/mol. From experimental data at 450, 500 and 550°C, the leak rate increase at 400°C was extrapolated. In order to corroborate the calculated rate at 400°C, a 4 μm thick composite Pd membrane, M-53, was studied for over 2,000 h in H_2 atmosphere. M-53 showed a H_2 permeance of 42 m^3/m^2 h $bar^{0.5}$, and an outstanding selectivity (H_2/He) higher than 22,000 over 2,200 h, which was in agreement with the calculated leak rate increase at 400°C. *AIChE J,* 54: 487–494, 2008
Keywords: Pd membranes, leaks, defects, sintering, selectivity

Introduction

Hydrogen separation and production technologies are essential for the increasing demand for hydrogen in the petroleum and petrochemical industries, and for fuel cells applications. Methane steam reforming is currently the major route for the production of H_2 in a large-scale production. The reaction, which requires large amounts of energy, takes place in tubular reactors at a temperature close to 800–900°C, with a yield of approximately 20%. Carrying out the same reaction in a H_2 permeable composite membrane reactor allows the use of lower temperatures (~500°C), higher yields (>95%), and the production of high-purity H_2, reducing investment and production costs. Pd and Pd alloy membranes are of preference due to their thermal and mechanical stability at the temperatures of 400–500°C, and their high-selectivity, theoretically infinite, for H_2.

A large number of composite Pd membranes have been prepared by many researchers on Al_2O_3 supports,[1–4] Vycor glass[5] and modified porous metal (PM) supports.[6–12] Many composite Pd membranes showed high H_2 permeance[5,7,10,13] and good long-term chemical stability. Indeed, even for composite Pd membranes on PM supports, new technologies have reduced to a large extent the problems posed by intermetallic diffusion.[14–16] However, leak stability over time at high-temperatures (T > 450°C) is an issue that have not received too much attention, but arises in almost all composite Pd membranes.

Guazzone et al.[18] attributed leak growth over a long period of time to the formation of pinholes on the surface of composite Pd membranes, which was also reported by Lee et al.[19] and Paglieri et al.[20] In fact, the formation of pinholes, the release of stresses and the growth of Pd grains were attributed to the sintering of Pd crystallites by Guazzone et al.[18]

Correspondence concerning this article should be addressed to Y. H. Ma at yhma@wpi.edu.

Table 1. Characteristics of Composite Pd Membranes

Membrane	Support type	Area (cm^2)	Pd thickness (μm)	Reference
C01-F11	PSS[1]	23	17	M3-a [24]
C01-F11b	C01-F11	23	19	M3-b [24]
M-32	PH[2]	120	7.7	This work
M-32b	M-32	120	10	This work
M-34	PH	120	4	This work
M-34b	Ma-34	120	8	This work
M-42	PH	120	5.6	This work
M-52	PH	120	2,8	This work
M-52b	PH	120	3.8	This work
M-53	PH	120	4	This work
M-54	PH	120	4	This work

[1]PSS = porous stainless steel.
[2]PH = porous hastelloy.

The main objective of this work was to investigate the process taking place at temperatures close to 400–450°C, that led to leak growth in many composite Pd membranes. The leak distribution on the surface was examined to determine whether leakage in composite Pd membranes was a localized phenomenon, or a process taking place over the entire surface of the membrane. The shape and size of defects were also studied. In addition, the rate at which the *He* leak of composite Pd membranes increased in H_2 atmosphere was measured at different temperatures to estimate the activation energy of the rate of the leak increase. The order of magnitude of the activation energy would provide information on the mechanism underlying the leak growth. Finally, a composite Pd membrane, M-53, was studied at 400°C over thousands of hours to corroborate the semiempirical leak model.

Experimental

Membrane preparation and characterization

Cylindrical porous metal supports for composite Pd membranes were prepared by welding to one end of the porous metal (PM) tube (2.54 cm OD, 15 cm long) a blind cap, and a nonporous metal tube to the other end. The weld nugget between the blind cap and the porous metal tube was denoted as the "lower weld" and the weld nugget between the porous metal tube, and the nonporous metal tube was denoted as the "upper weld". All porous metal supports were supplied by Mott Corporation, Farmington, CT, USA. Porous supports were cleaned, oxidized, graded, activated with Pd seeds, and electroless plated with Pd according to the experimental procedures described in our earlier publications.[21–23] The composite Pd membranes prepared are listed in Table 1, and were characterized in a H_2 permeation setup previously described by Guazzone et al.[24] The letter "b" after the name of membranes M-32/34 and 52 refers to repaired versions of the same membranes. That is, taking Ma-32 as an example, Ma-32 was characterized at all temperatures, removed from the reactor, repaired by replating and tested for a second time as Ma-32b. The repair consisted of the cleaning of the surface with acetone and Di-H_2O, the activation of the surface by the $SnCl_2$-$PdCl_2$ procedure, and the plating of 1 to 4 μm of Pd depending on the membrane. Hence, the repair did not affect the characteristics of the initial membrane besides the thickness, which was modified by addition of a fresh Pd layer. Generally, the H_2 permeance of all composite Pd membranes was determined at 250, 300, 350, 400, 450 and 500°C using H_2 gas with 99.95% purity. Permeate pressure was kept in all instances at atmospheric conditions.

Leak in composite Pd membranes

Since the leak in composite Pd membranes was measured with *He*, it was necessary to change the atmosphere from H_2 to *He*, and back from *He* to H_2. To determine the He leak (or the *He* permeance) at any given temperature, the *He* flux J_{He}, was measured at the following pressure differences: 1, 1.5, 2, 2.5, 3 and 3.5 bar. The He permeance was then determined by fitting the (J_{He}, ΔP) experimental data with Eq. 1

$$J_{He} = He_{\text{permeance}} \cdot \Delta P \tag{1}$$

where J_{He} is the He flux in $m^3/(m^2\ h)$, $He_{\text{permeance}}$ is the permeance of the *He* leak in $m^3/(m^2\ h\ bar)$, and ΔP is the pressure difference in bar. The ideal separation factor, denoted as selectivity (H_2/He), was defined by the ratio of the H_2 flux, J_{H2}, and the *He* flux J_{He}, at the same pressure difference and temperature. Since the H_2 flux was proportional to $\Delta(P^{0.5})$, and the He flux was proportional to ΔP, the selectivity (H_2/He) value depended on the pressure considered. In this work, all reported selectivities (H_2/He) were determined at a pressure difference of one bar (2:1) according to Eq. 2

$$\text{Selectivity } (H_2/He) = \left(\frac{J_{H_2}}{J_{He}}\right)_{\Delta P=1} = \frac{F_{0.5} \cdot (\sqrt{2}-\sqrt{1})}{He_{\text{permeance}} \cdot (2-1)} \tag{2}$$

where $F_{0.5}$ is the H_2 permeance determined assuming that Sieverts' law was valid (n = 0.5). In general, the *He* leak and selectivity (H_2/He) of the membranes were measured several times at 250, 300, 350, 400, 450 and 500°C.

The rate at which the He leak developed over time was determined by two methods: (1) by performing a linear regression on the (J_{He}, time) data when several leak measurements were taken at a given temperature, and (2) by performing the following calculation when only one leak measurement was taken at each temperature.

Figure 1 depicts the H_2 permeance as a function of time for an hypothetical membrane. At $t1$, He was introduced and the He leak at 450°C was measured. At $t2$, the temperature was changed from 450°C to 500°C at a rate of 1°C/min and at $t3$ the *He* leak at 500°C was measured. Based on experimental observations, the *He* leak did not evolve during the 50 min that were necessary to bring the temperature up by 50°C (e.g., from 450 to 500°C). Therefore, the *He* leak at point $t2$ was equal to the *He* leak at point $t1$ plus the increase in *He* leak that occurred at 450°C during the time $\Delta t = t2\text{-}t1$. Hence, the rate of increase for the leak at 500°C was given by Eq. 3

$$rHe_{500} = \frac{He(t3) - \{He(t1) + rHe_{450} \cdot (t2 - t1)\}}{t3 - t2} \tag{3}$$

where, $He(ti)$ is the *He* leak at the time ti (i = 1, 2, 3, etc.) and rHe_{temp} is the rate of increase for the *He* leak at the tem-

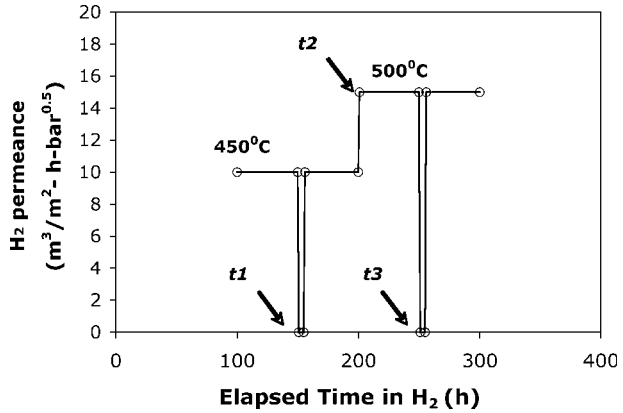

Figure 1. H_2 permeance vs. time for an hypothetical composite Pd membrane.

perature denoted in the subscript (temp). t_i corresponded to the time at which the *He* leak was measured, and the temperature was changed as shown in Figure 1.

Both methods for determining the *He* leak rate increase assumed the leak to increase linearly with time, which turned out to be a good approximation at temperatures equal to or higher than 450°C. The behavior of the leak at temperatures lower than 450°C was difficult to study since they grew at a very slow rate.

Leak distribution

After the completion of the H_2 permeation characterization at high-temperatures (500°C or higher), the large membranes (15 cm long, 2.54 cm OD, area = 120 cm^2) were cooled down to room-temperature and removed from the test unit. The distribution of the leak in these large membranes was measured by a "rising water" test.[25] It should be noted that the rising water tests were performed at the end of the characterization procedure, i.e., after having exposed the membrane to the highest temperature. The composite Pd membrane was housed in a Plexiglas shell, and sealed with rubber O rings. A scale, divided in cm, was printed on the wall of the Plexiglas tube. The membrane was placed in such a position that the lower weld matched with the "zero" mark of the printed scale; the 15th tick mark matched with the upper weld. A *He* gas cylinder was connected to the shell of the Plexiglas tube via a pressure regulator. A water reservoir was also connected to the shell of the Plexiglas tube. The tube of the membrane was connected to a gas-bubble-flow meter in order to measure the *He* flow at a given ΔP. Water was introduced cm by cm, and the *He* flux measured at every step. The details of the rising water test can be found in Guazzone's work.[7]

Results

Distribution of the leak in composite Pd membranes

Knowing the leak distribution in a composite Pd membrane was an important piece of information to understand whether the *He* leak was due to localized cracks, peeling off of the Pd layer or due to a process affecting the entire surface of the membrane.

The normalized *He* leak for membranes M-32b/34b/54/52 is plotted in Figure 2 as a function of the water level. The *He* leak of M-32b/54/52 membranes decreased rather evenly as the water level was increased, indicating that the *He* leak of the membranes was not localized and somewhat evenly distributed across the entire surface of the Pd layer. The slope of the line of leak vs. water level was not the same for all membranes since they were not tested in the same reactor, and the temperature gradient along the reactor axis might not have been the same. The *He* leak of M-34b shows a sharp decrease at the upper weld indicating the presence of a large defect at the welding between the nonporous and the porous part. When the leak at the weld was subtracted from the total leak, the *He* leak of M-34b ("M-34b corrected") followed the similar trend shown by M-32b. Leaks seldom appeared in the welds, and M-34b was a rare exception and was the consequence of a failure at the weld. The leak was generally well distributed over the surface of the membrane. Therefore, the process leading to the leak formation and leak growth affected the entire Pd layer.

Shape, location and size of defects

Since the leak was distributed over the entire surface of the membrane, analyzing the surface of a small portion of any given membrane gave a good representation of the entire surface of the membrane. The SEM analysis of several composite Pd membranes showed that the composite Pd membranes having leaks showed the presence of pinholes at their surface, which was previously reported.[18–20] Figure 3 shows the morphology of M-32b after the heat treatment at 550°C for 48 h in H_2 atmosphere. As reported earlier, fresh Pd deposits from electroless plating are characterized by Pd clusters including very small Pd crystallites (~50–100 nm).[18] Upon the heat treatment, crystallites grew within the clusters reaching sizes in the order of 1-2 μm. All Pd clusters in Figure 3 included visible large Pd crystallites 1-2 μm in size. Also, upon heating at high-temperatures, pinholes were formed, and were mainly found to be located at the boundaries of Pd clusters and Pd crystallites as pointed out by

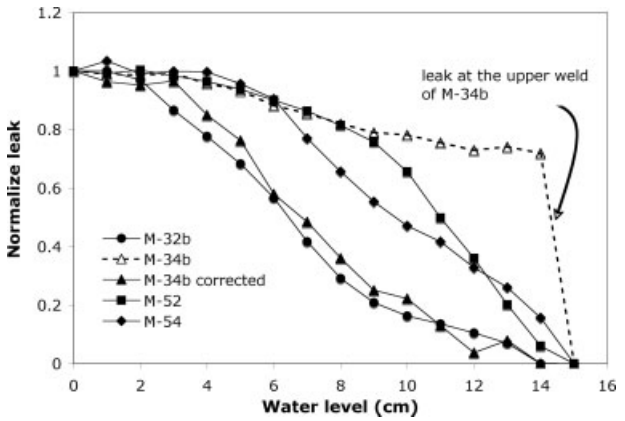

Figure 2. *He* leak as a function of water level for membranes M-32b/34b/52 and M-54 before and after H_2 test.

The "0" mark corresponds to the lower weld, and the "15" mark corresponds to the upper weld.

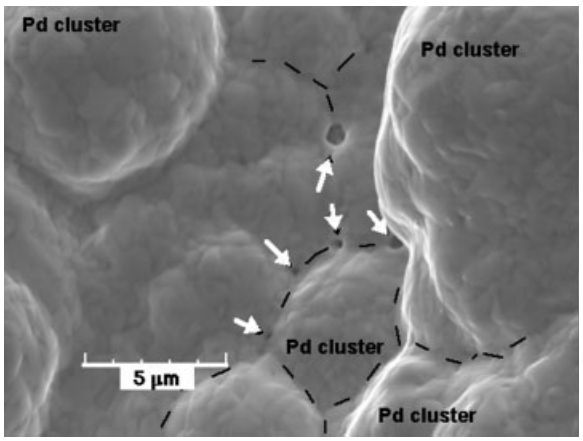

Figure 3. Surface morphology of M-32b after heat treatment at 550ºC for 48 h in H_2.

arrows in Figure 3, with the diameter of the largest pinhole being around 1μm. Smaller pinholes can also be seen in Figure 3.

The diffusion of *He* through the defects in a Pd layer can be approximately given by the sum of a Knudsen term and a viscous term (slip-flow) as shown in Eq. 4. The flux of inert gases through defects was modeled as the flux of gases through a porous media with a very small porosity.[7,21] Equation 4 assumes that the defects of composite Pd membranes were pinholes within the Pd layer with an average diam. d, and that the surface diffusion of gases is negligible.

$$\frac{J}{\Delta P} = \alpha + \beta \cdot P_{\text{ave}} = \frac{2}{6}\sqrt{\frac{8}{\pi}}\,\frac{\varepsilon \mu_k d}{L_{Pd}\sqrt{RTM}} + \frac{1}{32}\,\frac{\varepsilon \mu_v d^2}{L_{Pd}\eta RT}\cdot P_{\text{ave}} \tag{4}$$

In Eq. 4 $\alpha{\cdot}\Delta P$ is the Knudsen flow, $\beta{\cdot}\Delta P{\cdot}P_{\text{ave}}$ is the viscous flow, ε is the porosity, μ_k and μ_v are, respectively, the Knudsen and viscous geometric factor coefficients, d is the pore diameter in m, L_{Pd} the thickness of the Pd layer in m, R is the universal gas constant in kJ/(mol K), T the temperature in K, M the gas molecular weight in kg/mol, and η the gas viscosity in Pa·s. μ_v is equal to $1/\tau$ (τ being the tortuosity factor), and μ_k is equal to $1/(\tau\ \theta_k)$ with θ_k the reflection factor. The reflection factor is proportional to the roughness of the pore walls. Smooth walls are characterized by a θ_k value equal to 1, while rough surfaces have reflection factors greater than 1. Since pinhole walls were smooth, θ_k was assumed to be equal to 1; Therefore, μ_k equaled μ_v. Plotting gas permeance ($J/\Delta P$) as a function of the average transmembrane pressure led to a straight line with α as the y-intercept, and β as the slope. The average diameter d can be estimated from the β/α ratio given by Eq. 5

$$\frac{\beta}{\alpha} = \theta \cdot \frac{3}{32} \cdot \sqrt{\frac{\pi}{8}} \cdot \frac{1}{\sqrt{RT}} \cdot \frac{\sqrt{M}}{\eta} d \tag{5}$$

The accuracy achieved on the determination of the diameter depended on the accuracy with which the β/α ratio was measured, which was estimated to be 10–20%. The pinhole diameter was estimated with a 20% accuracy.

Table 2 summarizes the *He* leak, the selectivity (H_2/He), and the average pinhole size determined for each membrane after they were kept for a given amount of time at a given temperature. Membranes having a high-selectivity (H_2/He) (>800) were characterized by a very small average pinhole size equal to 0.16–0.17 μm, while membranes having a low-selectivity (<100) were characterized by an average pinhole size larger than a micron. It was then clear that the increase in the leak was related to the increase in the average size of the pinholes.

Therefore, from Figure 3 and Table 2, the formation of leaks in composite Pd membranes was attributed to the formation and growth of pinholes located at the boundaries of Pd clusters and/or Pd grains.

Kinetics of leak growth at 450–550°C in H_2

Figure 4a, b and c show the *He* leak as a function of time in H_2 atmosphere for membranes M-32b/34b/52b/54 at 450, 500 and 550°C, respectively. For almost all membranes, the *He* leak increased linearly with time except for M-32b (Figure 4b), which was characterized by a long induction time of 200–300 h. However, after the induction time, the *He* leak of Ma-32b was considered to increase linearly with time. The rate at which the *He* leak increased was deter-

Table 2. *He* Leak and Selectivity of all Membranes

Membrane	Temp. (°C)	Time spent at max Temp. (h)	H_2 permeance at Temp. (col. 2) (m^3/m^2-h-$bar^{0.5}$)	He leak. (m^3/m^2-h-bar)	Selectivity at ΔP = 1bar (H_2/He)	Average pinhole diameter (μm)
C01-F11	500	319	20.6	0.0125	683	0.83
C01-F11b	500	179	23.5	0.0214	478	0.47
C01-F11b	550	93	28.3	0.234 (at RT)	52	0.34
M-32	500	52	50	0.485	42	nd
M-32b	500	1100	41	0.0651	280	nd
M-32c	500	556	38	1.101 (at RT)	14	1.3
M-34b	500	552	20	0.0957	86	0.92
M-42	500	111	39	0.0165	980	0.04
M-42	500	185	39	0.019	818	0.16
M-52	500	275	94.2	0.591	66	nd
M-52b	450	260	55.5	0.0125	1806	2.7
M-53	400	2286	42.6	$7.78{\cdot}10^{-4}$	22000	nd
M-54	500	120	45.7	0.143	132	nd

nd = not determined.

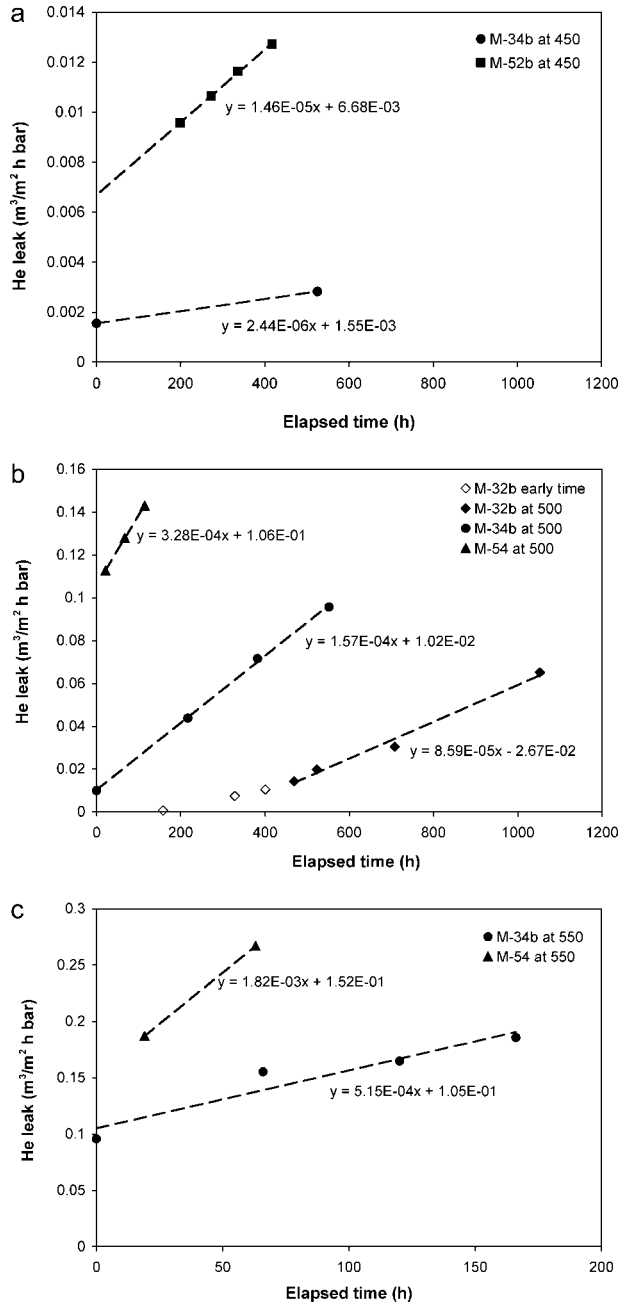

Figure 4. He leak rate increase in H_2 atmosphere at (a) 450°C for M-34b/52b, (b) 500°C for Ma-32b/34b/54, and (c) 550°C for membrane Ma-34b/54.

mined in all membranes by either (1) fitting the J_{He} vs. time data with a straight line, or (2) applying Eq. 3, when only one leak measurement per temperature was taken. For the case of M-32b, only the last four experimental data points were considered for the *He* leak rate increase determination. The rate at which the *He* leak increased in M-32b/34b/52b/54 is reported in Figure 4a, b and c, which was equal to the slope of the regression lines in $m^3/m^2\ h^2$ bar.

For all other membranes (C01-F11/11b, M-42/52) the rate at which the leak developed was calculated using the raw data listed in Table 3 and Eq. 3 is summarized in Table 3.

From the rates listed in Figure 4 and Table 3, it may be noted that at a given temperature the *He* leak did not increase with the same rate for all membranes. Thin membranes, M-52/54 developed a leak at a faster rate. Also, repaired membranes, M-32b/34b/52b, developed a leak at a slower rate than during their first H_2 test characterization. Figure 5 shows the rate at which the *He* leak increased for all membranes listed in Table 1 at 450, 500 and 550, as a function of membrane thickness. Although more experimental data are needed, it shows, as expected, that thinner membranes developed a leak at a faster rate than thicker membranes.

The natural logarithm of the rate of increase for the leak of all membranes was then plotted as a function of the reciprocal of temperature (Arrhenius plot), in order to estimate the activation energy of the mechanism underlying the leak growth in composite Pd membranes. The Arrhenius plot of the leak rate growth for membranes C01-F11a/11b and membranes M-32b/34b/42/52/52b/54 is shown in Figure 6. Since the leak hardly grew in the 250–400°C temperature range, the activation energy for leak growth was only estimated in the 450–550°C temperature range using the rate at which the leak increased for membranes C01-F11a/11b and M-32b/42. The data of M-34/52/54 were omitted for the calculation of the activation energy due to the low thickness of these membranes. The data of M-34b was omitted due to its failure at the upper weld (see Figure 2).

The activation energy for the rate of increase was estimated to be 238 kJ/mol, which closely matched the activation energy of Pd self-diffusion coefficient of 266 kJ/mol. Hence, the leak growth was a diffusion-limited process, which required the diffusion of Pd atoms.

At 400°C in H_2: the case of M-53

The rate at which the He leak increased at 400°C in composite Pd membranes was calculated by extrapolation using the equation on Figure 6, and equaled $4.47 \cdot 10^{-7}$ $m^3/m^2\ h^2$ bar. The sensitivity of the *He* mass flow meter used being 0.1 sccm, 1118 h would be needed to measure an increase of only 0.1 sccm at a transmembrane pressure of 1 bar. This is why the rate at which the He leak increased at temperatures lower than or equal to 400°C for all membranes in Figure 6 (except for M-53) was the same at 300, 350 and 400°C. In fact, except for M-53, not enough time was allowed for the leak to develop and measurements were inaccurate.

Membrane M-53 was prepared according to the procedure described by Ma and Guazzone[23] and characterized in order to experimentally verify the predicted behavior of the leak growth at 400°C. The cross-section of M-53, shown in Figure 7, indicated a very uniform and thin membrane. M-53, with an average of 4 μm in thickness, was tested in H_2 atmosphere at 400°C for over 2,200 h. The *He* leak before H_2 introduction ($t = 0$ h) was undetectable at 400°C, and at ΔP of 3.3 bars.

The *He* leak was measured every 160 h by switching from H_2 to *He* atmosphere at a He pressure difference of 3.3 bar in order to have a measurable *He* flux (>0.1 sccm). Figure 8 shows the H_2 permeance and selectivity (H_2/He) as a function of time at 400°C. The H_2 permeance slowly increased from 35 $m^3/m^2\ h\ bar^{0.5}$ at $t = 0$ h to 54.7 $m^3/m^2\ h\ bar^{0.5}$ at

Table 3. *He* Leak, and *He* Leak Rate Increase for all Composite Pd Membranes

	Temperature (°C)	Temp. change time (h)	Time leak (h)	He leak ($m^3/(m^2$ h bar))	Selectivity	He leak rate increase ($m^3/(m^2$ h^2 bar))
C01-F11a	450	576	725	1.497E-03	4989	5.337E-06
	450	576	730	1.417E-03	5235	4.644E-06
	500	820	990	1.250E-02	683	6.759E-05
C01-F11b	450	599	1020	8.297E-03	997	1.304E-05
	500	1042	1169	2.145E-02	478	1.013E-04
	550	1220	1395	2.340E-01	52	1.185E-03
M-32b	500			Linear regression		
M-34	500	0	150	6.971E-02	300	4.647E-04
M-34b	450	Linear regression. The rates at 500, and 550°C were considered for the Ea of leak growth since the				
	500	blister at the weld may have formed and grew in H_2 atmosphere at temperatures				
	550	equal to or higher than 500°C				
M-42	450	378	499	6.000E-03	2665	4.242E-05
	500	501	612	1.639E-02	980	9.286E-05
M-52	450			Linear regression		
	500	0	0	7.000E-02		
	500	0	284	5.917E-01	66	1.837E-03
M-53	400			Linear regression		
Ma-54	500			Linear regression		
	550					

t = 831 h. After 831 h the H_2 permeance started to slowly decline as a function of time. The decline in H_2 permeance was most probably due to a slight amount of intermetallic diffusion at the low-temperature of 400°C. The most important factor in M-53 was its leak stability. No *He* flux was detected after more than 1,100 h, time at which the first 0.06 sccm (ΔP = 1 bar) of *He* was measured. The selectivity (H_2/*He*) at t = 1,154 h equaled 72,000. After a minor incident (loss of H_2 pressure) where the membrane stayed for around 2 h in air at 400°C, the selectivity dropped to 25,000 at t = 1655 h. M-53 was finally put in *He* atmosphere after 2,286 h in H_2, and cooled down to room-temperature. The last *He* leak measurement at 400°C (t = 2227 h) equaled $7.87 \cdot 10^{-4}$ m^3/m^2 h bar, which corresponded to a selectivity (H_2/He) of 22,000. Figure 9 shows the *He* leak at 400°C as a function of time. The average rate at which the *He* leak increased was equal to $3.91 \cdot 10^{-7}$ m^3/m^2 h^2 bar, which was relatively close to the rate predicted by the equation in Figure 6 at 400°C of $4.47 \cdot 10^{-7}$ m^3/m^2 h^2 bar. In fact, the extrapolation of the 450–500°C regression line crosses the experimental point for M-53 at 400°C. Hence, it was experimentally demonstrated that composite Pd membranes prepared by the electroless deposition method do not develop leaks for long periods of time at temperatures lower than or equal to 400°C in H_2 atmosphere. Finally, during the H_2 test of M-53, the atmosphere was changed 14 times at 400°C without affecting the separation properties of the composite Pd membrane.

Discussion

Sudden leak formation in composite Pd membranes prepared by the electroless deposition method may occur due to: $\alpha \rightarrow \beta$ transformation caused by equipment failure,[18] peeling off of the Pd layer,[26] or failure at the welds between porous parts and nonporous parts. However, for all membranes listed in Table 1, care was taken to remain in the stability region of the α Pd-H phase, no peeling off of the Pd layer was

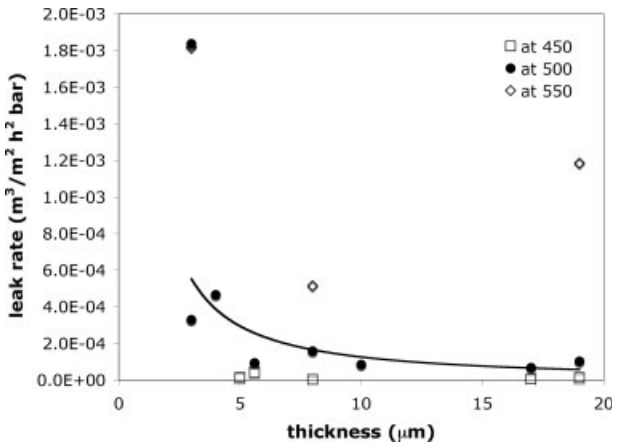

Figure 5. Rate at which the *He* leak increased as a function of membrane thickness.

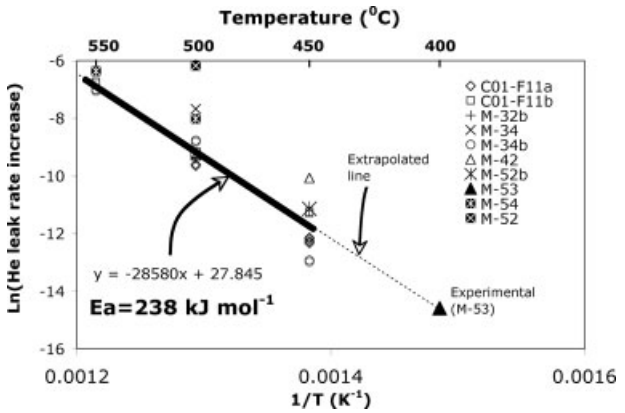

Figure 6. Arrhenius plot for membranes C01-F11a/11b and membranes M-32b/34/34b/42/52/52b/53/54.

The activation energy was only estimated in the 450–550°C temperature range.

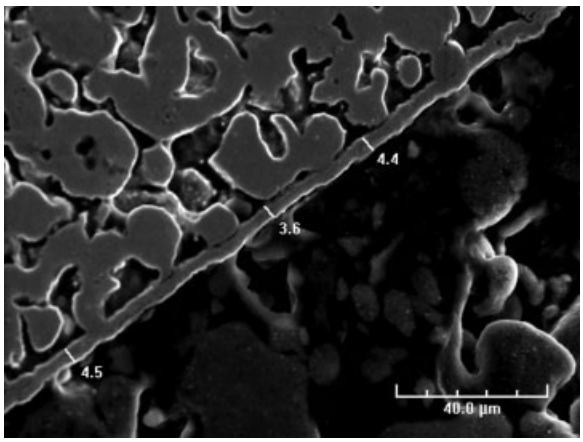

Figure 7. Cross-section of M-53.

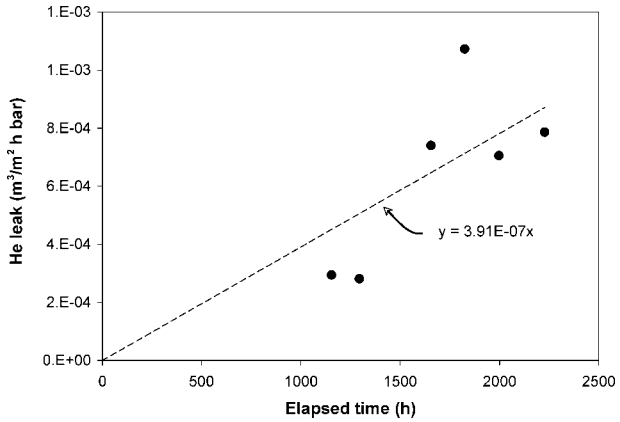

Figure 9. *He* leak of M-53 as a function of time at 400ºC.

observed and, except for the case of M-34b, the rising water test result of all membranes indicated no failure at the welds. Yet, the He leak gradually grew with time and was always distributed over the entire surface of the composite Pd membrane. The leak grew due to the formation and growth of pinholes, which was supported by the fact that pinholes were observed on the surface of Pd membranes, and the composite Pd membranes with a larger leak had larger pinholes at their surface.

The high-activation energy of 238 kJ/mol for the leak growth indicates that pinhole formation is a diffusion-limited process. Moreover, as already stated, the activation energy for leak growth was very close to the activation energy of Pd self-diffusion coefficient of 266 kJ/mol. Hence, pinhole formation and growth was related to the movement of Pd atoms. An activation energy of 238 kJ/mol is characteristic of sintering processes, which is in many cases diffusion limited (at low-temperatures). Sintering can occur coherently and incoherently.[27] Coherent sintering leads to a homogeneous and high-density (close to or equal to the bulk material) material. However, incoherent sintering leads to evolution of pores and microholes due to local densification or differential shrinkage. Differential shrinkage is characteristic of sintering in ultrafine materials.[27]

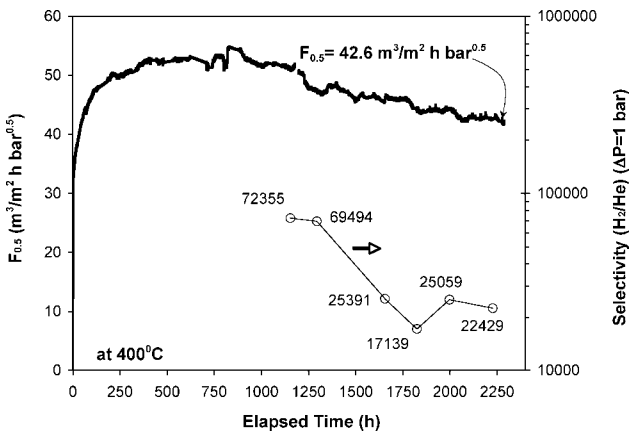

Figure 8. H_2 permeance and selectivity (H_2/He) of M-53 at 400ºC.

Hence, the tendency to form leaks in composite Pd membranes prepared by the electroless deposited method may be explained by the fact that fresh electroless Pd deposits are characterized by a relatively high-driving force for sintering due to their fine grain structure (100 nm Pd crystallites), small Pd clusters,[18] and their relatively small porosity incorporated within the film.[28] Also, leak development in "well prepared" fresh composite Pd membranes having their Pd layer deposited by the electroless deposition method will always, and in an inherently manner, occur at temperatures higher than 400–450°C. The term "well prepared" refers to composite Pd membranes synthesized with care, having no initial *He* leak and no local defects, such as the formation of the leak in a single spot as seen in M-34b at its upper weld. In other words, the mechanism leading to leak formation was the incoherent sintering of Pd clusters and/or Pd grains.

However, sintering at 400°C occurred at a slow rate, and this work experimentally showed that composite Pd membranes prepared by the electroless method have a great potential for industrial applications at temperatures close to 400°C. The ideal separation factor (H_2/He) of membrane M-53 was characterized by an outstanding stability, since it was higher than 22,000 for over 2,200 h in H_2 atmosphere. Furthermore, if membranes are thin, high H_2 permeances could be achieved at 400°C since M-53 showed a high H_2 permeance equal to 42.6 m^3/m^2 h $bar^{0.5}$ after 2,286 h at 400°C. We believe that temperature may affect leaks in a more detrimental manner than thickness. Therefore, thin membranes (2-3 μm) may have high H_2 permeances and still be selective for long periods of time at 350–400°C.

Conclusions

The leak in composite Pd membranes was distributed over the entire surface, and was due to the formation and growth of pinholes at the Pd clusters and Pd crystallites boundaries. The mechanism for leak growth was found to be a diffusion-limited process with an activation energy equal to 238 kJ/mol, which corresponded to the activation energy of Pd self-diffusion coefficient. Pinhole formation at temperatures higher than 400–450°C was attributed to the incoherent sintering of the small Pd clusters and/or Pd crystallites. The outstanding selectivity (H_2/He) stability of M-53, which was

higher than 22,000 over 2,200 h, demonstrated that H_2 with a purity over 99.999% could be obtained with composite Pd membranes prepared by the electroless deposition method in processes where temperatures are close to 400°C. Finally, the empirical equation developed in this work can be used as a guideline for accelerated tests of the leak stability of a membrane at a lower-temperature.

Acknowledgments

The authors would like to thank the financial support provided by Shell International Exploration and Production, Inc. and Shell Hydrogen. Also, the setup and concepts used for the rising water test experiments were kindly communicated to us by the research team at Shell International Exploration and Production, Inc., Huston, TX.

Literature cited

1. Pan X, Kilgus M, Goldbach A. Low-temperature H_2 and N_2 transport through thin $Pd_{66}Cu_{34}H_x$ layers. *Catalysis Today*. 2005;104: 225–230.
2. Roa F, Way JD, McCormick RL, Paglieri SN. Preparation and characterization of Pd-Cu composite membranes for hydrogen separation. *Chem Eng J*. 2003;93:11–22.
3. Sun GB, Hidajat K, Kawi S. Ultra thin Pd membrane on α-Al_2O_3 hollow fiber by electroless plating: High permeance and selectivity. *J of Membr Sci*. 2006;284:110–119.
4. Wang WP, Thomas S, Zhang XL, Pan XL, Yang WS, Xiong GX. H_2/N_2 gaseous mixture separation in dense Pd/α-Al_2O_3 hollow fiber membranes: Experimental and simulation studies. *Sep and Pur Technol*. 2006;52:177–185.
5. Uemiya S, Sato N, Ando H, Kude Y, Matsuda T, Kikuchi E. Separation of hydrogen through palladium thin film supported on a porous glass tube. *J of Membr Sci*. 1991;56:303–313.
6. Checchetto R, Bazzanella N, Patton B, Miotello A. Palladium membranes prepared by r.f. magnetron sputtering for hydrogen purification. *Surface and Coatings Technol*. 2004;177–178:73–79.
7. Guazzone F. Engineering of substrate surface for the synthesis of ultrathin composite Pd and Pd-Cu membranes for H_2 separation. Worcester Polytechnic Institute, Worcester MA; 2006. PhD Dissertation.
8. Tong J, Kashima Y, Shirai R, Suda H, Matsumura Y. Thin defect-free pd membrane deposited on asymmetric porous stainless steel substrate. *Ind & Eng Chem Res*. 2005;44:8025–8032.
9. Tong J, Su C, Kuraoka K, Suda H, Matsumura Y. Preparation of thin Pd membrane on CeO_2-modified porous metal by a combined method of electroless plating and chemical vapor deposition. *J of Membr Sci*. 2006;269:101–108.
10. Tong J, Suda H, Haraya K, Matsumura Y. A novel method for the preparation of thin dense Pd membrane on macroporous stainless steel tube filter. *J of Membr Sci*. 2005;260:10–18.
11. Wang D, Tong J, Xu H, Matsumura Y. Preparation of palladium membrane over porous stainless steel tube modified with zirconium oxide. *Catalysis Today*. 2004;93–95:689–693.
12. Klette H, Bredesen R. Sputtering of very thin palladium-alloy hydrogen separation membranes. *Membr Technol*. 2005;2005:7–9.
13. Su C, Jin T, Kuraoka K, Matsumura Y, Yazawa T. Thin palladium film supported on SiO_2-modified porous stainless steel for a high-hydrogen-flux membrane. *Ind & Eng Chem Res*. 2005;44:3053–3058.
14. Mardilovich IP, Engwall EE, Ma YH. Thermally stable composite Pd membranes having intermediate porous metal intermetallic diffusion barrier layers formed by bi-metal multi-layer deposition. Ninth International Conference on Inorganic Membranes (ICIM9). Lillehammer, Norway; June 25–29, 2006.
15. Nam S-E, Lee K-H. Hydrogen separation by Pd alloy composite membranes: introduction of diffusion barrier. *J of Membr Sci*. 2001; 192:177–185.
16. Nam SE, Lee KH. Preparation and characterization of palladium alloy composite membranes with a diffusion barrier for hydrogen separation. *Ind & Eng Chem Res*. 2005;44:100–105.
17. Lewis FA. *The Palladium-Hydrogen System*. Lewis FA, ed. London, New York: Academic Press; 1967.
18. Guazzone F, Speakman AS, Payzant EA, Ma YH. Microstrains and stresses analysis in electroless deposited thin Pd films. *Ind & Eng Chem Res*. 2006;45:8145–8153.
19. Lee D-W, Lee Y-G, Nam S-E, Ihm S-K, Lee K-H. Study on the variation of morphology and separation behavior of the stainless steel supported membranes at high temperature. *J of Membr Sci*. 2003; 220:137–153.
20. Paglieri SN, Foo KY, Way JD, Collins JP, Harper-Nixon DL. A new preparation technique for pd/alumina membranes with enhanced high-temperature stability. *Ind & Eng Chem Res*. 1999;38:1925–1936.
21. Mardilovich PP, She Y, Ma YH, Rei M-H. Defect-free palladium membranes on porous stainless-steel support. *AIChE J*. 1998;44: 310–322.
22. Ma YH, Mardilovich PP, She Y. Hydrogen gas-extraction module and method of fabrication. US patent 6,152,987. 2000.
23. Ma YH, Guazzone F. Composite gas separation modules having a layer of particles with a uniform binder metal distribution. US patent application 2006016332. 2006.
24. Guazzone F, Engwall EE, Ma YH. Effects of surface activity, defects and mass transfer on hydrogen permeance and n-value in composite palladium-porous stainless steel membranes. *Catalysis Today*. 2006;118:24–31.
25. Kreitman K, Matzakos AN. *Rising water test. Personal communication*. Shell: Houston, TX; 2005
26. Thoen PM, Roa F, Way JD. High flux palladium-copper composite membranes for hydrogen separations. *Desalination*. 2006;193:224–229.
27. Skorokhod VV. Surface relaxation and local densification in nanosized systems at isothermal sintering. Sintering 2003: An International Conference on the Science, Technology & Applicaltions of Sintering. State College, PA; September 15–17, 2003.
28. Yang RP, Cai X, Chen QL. Mechanism of hydrogen desorption during palladium brush-plating. *Surface and Coatings Technol*. 2001; 141:283–285.

Manuscript received Mar. 6, 2007, revision received Aug. 27, 2007 and final revision received Nov. 20, 2007.